

MODELING AND BISTATIC SIMULATION OF A HIGH RESOLUTION 3D PMD-CAMERA

Valerij Peters, Otmar Loffeld, Klaus Hartmann, Stefan Knedlik

Center for Sensor Systems (ZESS)

University of Siegen

Paul-Bonatz-Str. 9-11

57068 Siegen, Germany

Tel. + 49 271 740 2761

FAX + 49 271 740 2336

peters@zess.uni-siegen.de (Valerij Peters)

Abstract

To reduce the extent of the bistatic and other negative effects caused by the spatially separated illuminator and receiver positions in real 3D cameras, noiseless reference camera data are necessary. Such bistatic reference 3D data can be very helpful and in some applications indispensable for adaptive correction of the bistatic deformation. Due to the fact that the bistatic deformation effects cannot be individually separated from the total noise path (superposition of many noise types like thermal noise of the sensor, pixel size inequalities, etc.), such reference noiseless data can be generated only by means of simulations.

This paper presents a bistatic modeling and simulation approach for a high resolution 3D PMD camera.

At first, the paper describes a simulator for the monostatic case, which has been developed at the University of Siegen's Center for Sensor Systems. The simulator allows the user to calculate the theoretical response of a PMD sensor for a given 3D scene, referenced to absolute coordinates, so that the output of the simulator is comparable to real PMD sensor data. An advantage is that dynamic and static sensor parameters such as resolution, modulation frequency, fill factor, lens characteristics, sensor inclination and tilt, etc. can be at any time modified by the user.

The second part is concerned with the modeling and simulation of bistatic reference 3D data in the case of different positions of illuminator and sensor. The results of the simulated scenario including an error analysis are discussed.

Keywords: PMD; Photonic Mixing Device; Simulation; Modeling; Bistatic

Presenting Author's biography

Valerij Peters received the Diploma degree in electrical engineering from the University of Siegen in 2002. He is currently scientific assistant in the Center of Sensor Systems (ZESS) at the University of Siegen. His current research interests include 3D Vision, mono- and bistatic signal theory, multi sensor data fusion, computer based 2D and 3D sensor simulations.



1 Introduction

In recent years the progress in high-speed technical 3D-Vision development aroused increasing interest in many industrial, automotive and safety-related applications. Especially the newest 3D camera generation with an available resolution of up to 25.000 pixels (e.g. PMD[vision]® 19k, SwissRanger SR-3000) and the ability to capture the entire environment in three dimensions opens up completely new possibilities for many new kinds of applications in the areas of biometrics, mobile robotics, machine vision, navigation, positioning etc. In some of these applications very high 3D resolution is required. In such cases even the currently available all-solid-state solutions on the market today are sometimes not sufficient to meet the demands of the customers. According to the functional principle, construction and chip layout, 3D cameras with VGA resolution or higher at affordable prices are (at the moment) not available.

A promising solution of fast real-time 3D-perception is the combination of a high resolution 2D CCD camera and a lower resolution PMD¹ camera, which is under development in ZESS [1],[2]. The first prototype of such a hybrid 3D camera, which was introduced in ZESS at the end of 2006, provides 10-times the resolution of the PMD camera (VGA, 640x480 pixels).

The proposed PMD based 3D imaging systems offer following advantages over other existing 3D vision technologies such as stereo vision techniques or laser scanning:

- the 3D PMD camera delivers in one step depth information as well as gray values for each pixel (actual available sensor with 160x120 pixel)
- through the combination with a high resolution 2D CCD sensor the angle resolution can be improved considerably (actual available system with 640x480 pixel)
- high frame rate (up to 50 fps) and accuracy (<1cm) are feasible
- onboard illumination (infrared) → integrated on-chip suppression background illumination, i.e. operation largely independent of lighting environment and weather conditions
- low-cost production

The focus of development of a high-resolution, high-speed vision system is, among other things, put on the image registration and preferably distance-independent accuracy [3]. Especially the latter poses a challenge. Because of the construction-conditioned bistatic constellation of the PMD camera with the sensor and the illuminator, which is mounted outside of the camera, the formula

$$R = \frac{c \cdot t_{\text{delay}}}{2}$$

does not produce the correct result (with R – distance between camera and target object, c – speed of flight, t_{delay} – time of flight of the transmitted signal). This equation represents an approximation, which is valid only for large distances. In the common case the measured time of flight is represented by the sum of the time of flight from sensor to object and back from object to illuminator. That means the whole distance

$$\begin{aligned} \overline{IP} + \overline{PS} = & \sqrt{P_x^2 + (I_y - P_y)^2 + (I_z - P_z)^2} \\ & + \sqrt{P_x^2 + (P_y - S_y)^2 + (P_z - S_z)^2} \end{aligned}$$

will be measured (Fig. 2). The distances \overline{IP} and \overline{PS} are **unknown**.

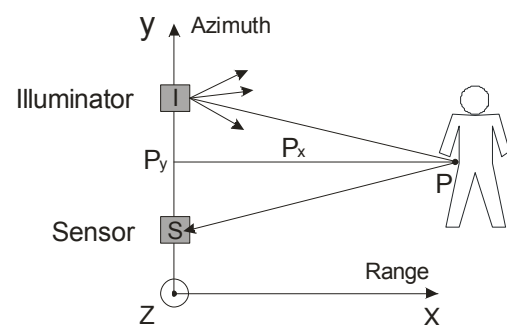


Fig. 1: Bistatic constellation of the sensor and illuminator

$P = (P_x, P_y, P_z)^T$ - position of the point target;

$I = (I_x, I_y, I_z)^T$ - position of the illuminator;

$S = (S_x, S_y, S_z)^T$ - position of the sensor;

For obtaining accurate estimates of the position of the target point (object) the bistatic equation has to be solved. A promising approach has been presented in [4]. To reduce the extent of the bistatic and other negative effects caused by the specific geometrical arrangement noiseless reference camera data are necessary. Due to the fact that bistatic deformation effects cannot be individually separated from the total noise path (superposition of many noise types like thermal noise of the sensor, pixel size inequalities, etc.), such reference data can be generated only by means of simulations. Such a PMD camera simulator as it is under development at ZESS and offers the following additional advantages:

- realistic modelling and simulation of mono-, bi- and multistatic PMD sensor scenarios
- simulation of different sensor geometries and constructive designs
- flexible parameterization and simulation of dynamic sensor properties like resolution, pixel sizes, modulation frequency, inclination, focal point etc.
- simulation in the loop etc.

¹ PMD (Photonic Mixer Device) is a 3D imaging sensor, developed in ZESS at the University of Siegen.

This paper presents a simulation approach for a high resolution 3D PMD camera.

2 Approach

2.1 “Monostatic” Simulation of a PMD Camera

The Photonic Mixer Device camera is based on CMOS technology with the additional possibility to measure the phase delay of reflected RF-modulated light, which is transmitted by an active onboard illumination unit with the wavelength usually in the infrared range. Due to the integrated internationally patented SBI (Suppression of Background Illumination) circuitry, the influence of interfering ambient light can be suppressed. These features allow the realization of robust and accurate outdoor 3D cameras.

The PMD camera consists of three main components, the PMD sensor itself, optics and illuminator. Initially in the following we assume a point illuminator, which is located at the same position as the sensor (monostatic configuration). Bistatic effects as a result of different positions of illuminator and sensor will be considered in the next chapter. In Fig. 2 the principle of a spherical biconvex lens is presented.

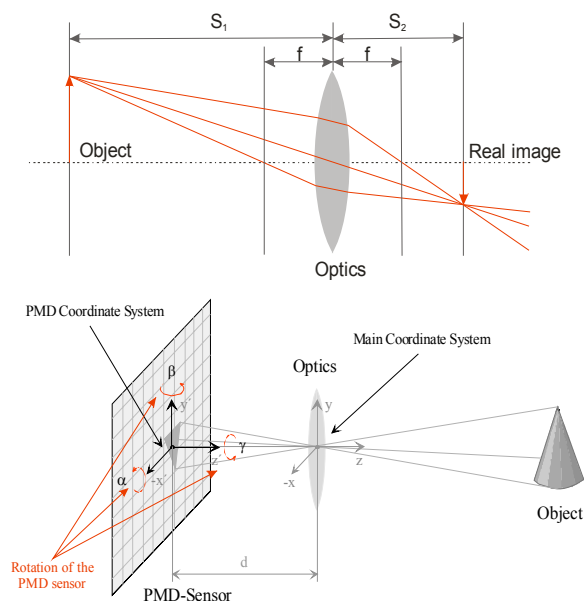


Fig. 2: a) Principle of biconvex lens b) Coordinate systems of the PMD camera

Defining the distances from the object to the lens and from the lens to the image as S_1 and S_2 respectively, the focal point for a lens of negligible thickness is given by the thin lens formula: $S_1^{-1} + S_2^{-1} = f^{-1}$. With an object placed at a distance S_1 along the axis in front of a positive lens of focal length f , a screen placed at a distance S_2 behind the lens will show an image of the object projected onto it, as long as $S_1 \geq f$. Obviously the whole optics can be described with a pinhole

camera positioned in the middle of the lens on the distance $d=S_2$. In the case of using other lens types the mapping algorithm has to be adapted accordingly.

To describe the camera's geometry we define two coordinate systems as shown in Fig. 2b). The main coordinate system is defined as follows: the point of origin is in the center of the lens (optics), the x-y plane lies in the lens plane and the z-axis is directed to the front of the camera. To consider potential inclination or adjustments of the sensor chip relative to the optics and enable tests on non-ideal calibration conditions the PMD coordinate system is introduced, in which the x- and the y-axis are parallel to the edges of the PMD pixel matrix and the z-axis is directed as above. The transformation of a vector from the PMD coordinate system into the main coordinate system is given by

$$\begin{bmatrix} x & y & z \end{bmatrix}^T = D_1(\alpha) \cdot D_2(\beta) \cdot D_3(\gamma) \cdot \begin{bmatrix} x' & y' & z' \end{bmatrix}^T + \vec{t} \quad (1)$$

with \vec{t} = translation vector – difference in position between the points of origin and D_x = rotation matrices around the specified axis.

The purpose of the software-based simulator, which is currently under development in ZESS, is the pixelwise response calculation for a given 3D scene defined in form of points or polygons. The principle is expatiated in section 2.3. At first we consider the theoretical sensor response for a given synthetic 3D environment.

Theoretical response of the “monostatic” PMD sensor:

The principle of the PMD distance measuring system is based on the measurement of the time-of-flight τ_L of the transmitted signal, which leads to the distance to the object:

$$R = \frac{c \cdot \tau_L}{2} \quad \text{with } c = \text{speed of light}$$

Assuming continuous sinusoidal or rectangular modulation the distance is

$$R = \frac{c \cdot \Delta\varphi}{4 \cdot \pi \cdot f_{\text{mod}}} \quad (2)$$

with f_{mod} = modulation frequency and phase delay $\Delta\varphi = 2 \cdot \pi \cdot f_{\text{mod}} \cdot \tau_L$

The theoretical response of a pixel can be expressed by:

$$\vec{r}_c = \sum_{n=1}^N B_n \cdot e^{j4\pi \frac{r_n}{\lambda}} \quad (3)$$

, where $\lambda = \frac{c}{f_{\text{mod}}}$ is the wave length of the modulated

signal, B_n = backscatter coefficient of the point n (including signal propagation attenuation), $\vec{r}_n = [x_n \ y_n \ z_n]$ = distance vectors to all visible 3D object points, with $n=1 \dots N$.

Thus, the response of one pixel is a vector whose direction is the same as that of the vector from the

origin of the main coordinate system to the center of the angle of beam spread (Fig. 3).

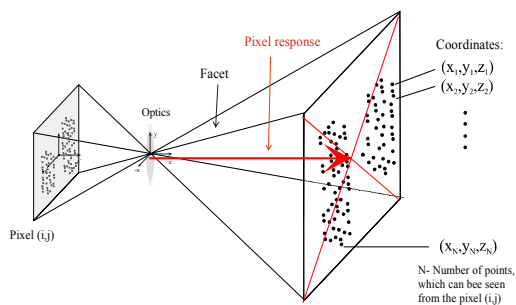


Fig. 3: PMD pixel response

Its absolute value can be calculated from the time of flight of the signal. A PMD sensor is not able to distinguish single points, which are located in the beam spread. Comparably to a CCD or conventional CMOS sensor, each pixel superimposes all returns from all imaged object points. Hence, as the pixel's output we obtain a "mixed" distance (phase) and brightness (amplitude of the signal) image:

$$\text{Amplitude: } A_m = |\vec{r}_c| \quad \text{Phase: } \varphi = \arg(\vec{r}_c) \quad (4)$$

2.2 "Bistatic" Simulation of a PMD Camera

In real PMD cameras the illuminator's size is too large to be implemented on chip and, as mentioned above, mostly mounted outside on the camera body. Fig. 4 shows an example for a possible illumination diodes layout (circular layout). The advantage of this layout compared to other common layouts is the approximately constant tangential illumination.

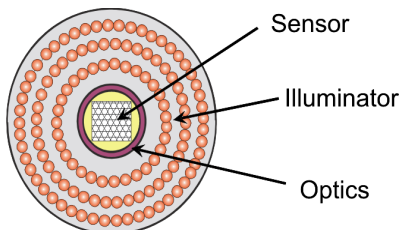


Fig. 4: System concept² and simulation approach of a real inhomogeneous illuminator

The radial intensity of the beam produced by the illumination diodes is represented by the overlapping

² 2D/3D camera for real-time applications developed in ZESS

of all single diode intensities, which are not uniform. Fig. 5 gives an example of such an infrared diode.

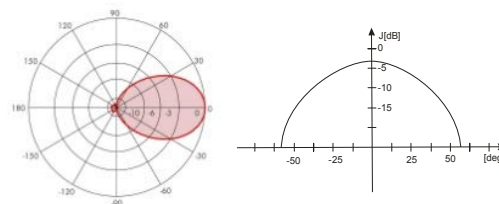


Fig. 5: Example: illumination diagram of infrared diode

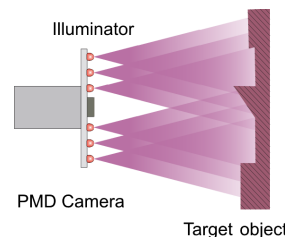


Fig. 6: Moire effect due to the non-uniform illumination

Thus, the intensity of the illuminated light depends on the angle to the point target. In the following we assume the whole PMD camera illuminator as a number of emitting point illuminators. That is each light emitting diode is represented by an idealized point light source with the appropriate illumination diagram. According to this, the illumination intensity at an arbitrary point target is with (2) on the one hand a function of the distance between the illuminator and the point target \overline{IP} , and on the other hand a function of the point target location. To calculate the theoretical response of a pixel we need to consider all possible light source point target interactions (Fig. 6). The light intensity at the point P is given by

$$I(P) = \sum_{m=1}^M I_m \cdot \frac{J_m(P)}{r_{I_m P}^2} \quad (5)$$

with I_m = specific damping factor of the light emitting diode m (depending on the quality of the diode, characteristics of the optical wave propagation medium etc.). $J_m(P)$ is the diagram based value of the illumination in the direction of the vector $\vec{r}_{I_m P}$. M is equal to the number of light sources, which can illuminate the point P. The theoretical pixel response of the combination of all visible (detectable) points P_n with the illuminator m can be expressed by:

$$\vec{r}_{c,m} = \sum_{n=1}^N B_n^* \cdot I_m \cdot \frac{J_m(P_n)}{r_{I_m P_n}^2} \cdot e^{j2\pi \frac{r_{I_m P_n} + r_{P_n S}}{\lambda}} \quad (6)$$

with $r_{I_m P_n}$ = distance between the illuminator m and the point P_n , $r_{P_n S}$ = distance between the point P_n and the pixel, B_n^* = specific backscatter coefficient of the

corresponding considered components. The overall pixel response represents the superposition of all possible illuminator-sensor interactions

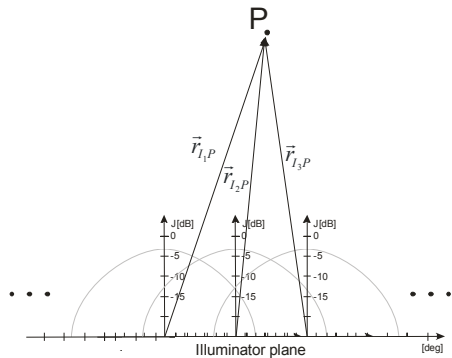


Fig. 7: Light source - point target interactions and can be expressed by

$$\vec{r}_c = \sum_{m=1}^M \vec{r}_{c,m} \quad (7)$$

2.3 Simulator architecture and realization

The actual release of the simulator is composed of some conditioning, editing and simulation units, which are schematically presented in Fig. 8.

Due to the limited paper length we restrict ourselves to the most important parts. To calculate the PMD camera response the following points are required:

- Sensor setup and parameterization → resolution, pixel size, filling factor, modulation frequency, lens characteristics, sensor inclination and tilt in respect to the main optical axis. In the monostatic illuminator-sensor configuration the position of the point light source can be defined by user. In the bistatic case the illuminator layout dataset with positions of all illumination diodes with their illumination characteristics are required.
- Visibility control unit which is responsible for the software-based rendering → All 3D geometry are available as primitives (points, triangles, quads, ...) in form of vertex/normal/texture coordinate lists (vertex streams) with corresponding index lists and shader status. For the observer the whole scene represents primarily just a congeries of points.

The main task is to separate the “visible” part of the scene in the view field of the camera. The blended parts, parts outside of the camera’s view field and the shadow side must be excluded in the point set P_n (cf. (6)). This can be done by means of hardware or software renderer. In our simulator we used a software-based Hidden Surface Removal (HSR) solution.

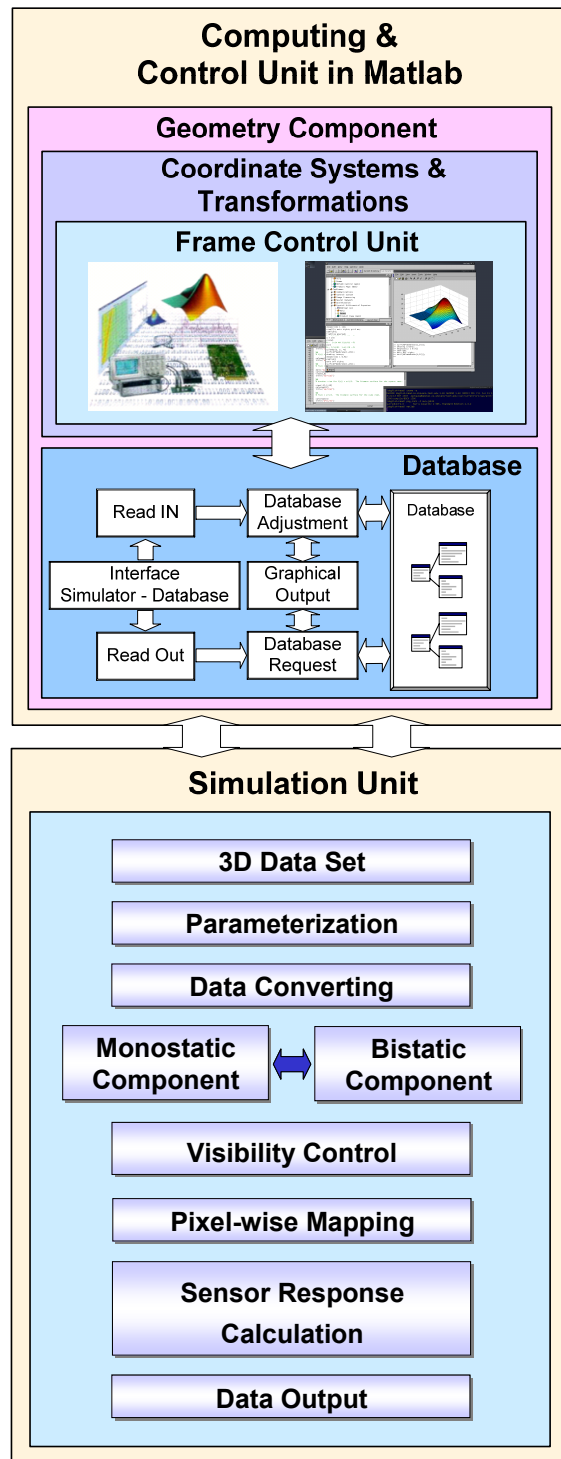


Fig. 8: PMD simulator architecture

- According to the illuminator kind, the sensor response will be calculated pixel-wise by using (4) and (7) respectively. Before this process can be applied, due to the fact, that for the response calculation from the pixel (i,j) all detectable object parts are required, all visible points/polygons have to be assigned to the corresponding pixel. Fig. 9 illustrates the assignment process in the case of a 2x2 pixel sensor with a spherical biconvex lens.

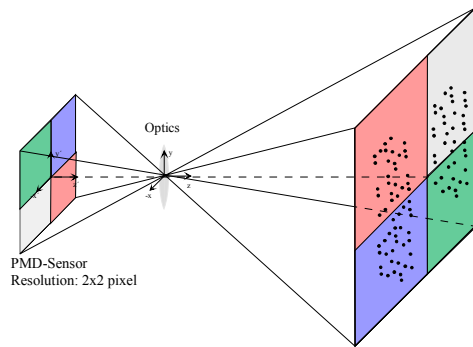


Fig. 9: Illustration of dynamic pixel-wise assignment of visible points

The pixels and the coverage areas which are belong to the appropriate pixels are identified with the same colour. The mapping and sorting process has been implemented in the mapping unit.

- The geometry module and the coordinate systems module are responsible for the navigation and orientation of the camera in the simulations. The frame control unit controls frame-wise
- In simulations of dynamic changeable and moving 3D scenes and in further releases also multiple camera systems, the environment and the camera properties can be frame-wise changed. This process will be controlled from the frame control unit.

3 First Bistatic Simulation Results

This section presents first simulation results for two bistatic illuminator constellations. The first constellation correspond with the camera construction presented in Fig. 4, which consists of 240 circular ordered idealized diodes (point light sources) and a 640x640 pixel PMD sensor.

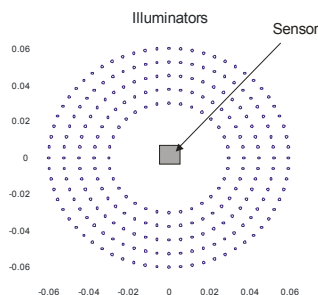


Fig. 10: Ring illuminator (5 diode rings with 240 diodes)

In the first approximation, the illuminator can be considered as a ring light source. The sensor is located in the middle of the ring illuminator and 'looks' perpendicular to the illuminator plane. As target object we used a barrier (wall) with the size of 0,4x0,4m at the distance of 2m. The midpoint of the barrier lies on the sensor optical axis. Fig. 11 presents the difference

between the simulated bistatic and monostatic sensor response for the given scene as greyscale.

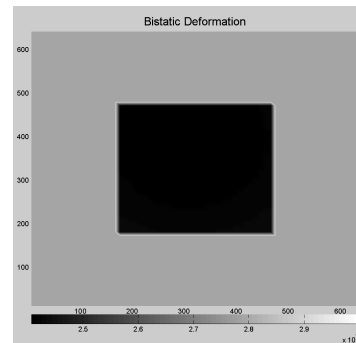


Fig. 11: Bistatic deformation in the case of ring illuminator

One can see that the bistatic deformation over the sensor is nearly constant and amounts 2,7mm. The error increases with increasing (bistatic range³)/(distance to the object) ratio (not shown here). In the second case to demonstrate the influence of the illuminator position and its form a half of the ring illuminator has been switched off (Fig. 12). That is only the light sources on the right side $[-\pi/2 \leq \alpha \leq \pi/2]$ were active.

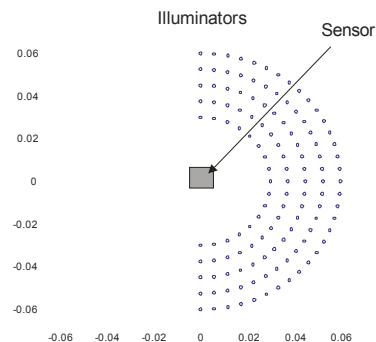


Fig. 12: Ring segment illuminator

In this simulation the error trend is much more pronounced (cf. Fig. 13). The absolute error reaches the maximum value on the illuminator closed and the opposed side and its minimum in the middle (center columns) of the sensor. The error ranges between -3 and 5mm.

³ Bistatic range – distance between the sensor and the illuminator

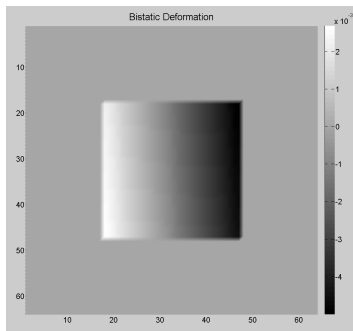


Fig. 13: Bistatic deformation in the case of ring segment illuminator

4 Conclusions and Future Works

This paper presents a software-based simulation approach of a 3D PMD camera, which enables calculating the theoretical sensor response. The PMD simulator, which is under development in ZESS, allows in its current form and state of development to generate simulated monostatic and also bistatic reference data.

The first simulation results illustrate the influence of the bistatic deformation, which is reflected in a measurement error in real camera systems. In the shown examples the bistatic error was comparatively small. The background emission and internal noises are a dimension higher as the bistatic error. But with increasing (bistatic range)/(distance to the object) ratio the bistatic influence becomes more important and has to be investigated especially in near range applications.

Future work will focus on refinements of the simulator, including arbitrary camera and illumination position and orientation in 3D up to multiple camera and illuminator systems. Furthermore the simulation results will be compared and verified with real measurement data.

5 References

- [1] T.D.A. Prasad, K. Hartmann, W. Wolfgang, S.E. Ghobadi, A. Sluiter. First steps in enhancing 3D vision technique using 2D/3D sensors. Computer Vision Winter Workshop 2006, Telc, Czech Republic, February 6–8, 2006
- [2] A. Rasool, K. Hartmann, W. Weihs. First Step in Implementing a Feature-based Stereo Algorithm in a Cost Efficient Way using a PMD Sensor. Visualization, Imaging and Image Processing, Palma de Mallorca, Spain, August 28-30, 2006
- [3] M. Lindner, A. Kolb. Lateral and Depth Calibration of PMD-Distance Sensors. International Symposium on Visual Computing (ISVC06), Advances in Visual Computing, Lake Tahoe, Nevada, Nov 6-8, 2006

- [4] O. Loffeld, H. Nies, V. Peters, S. Knedlik. Models and Useful Relations for Bistatic SAR Processing. IEEE Trans. Geosci. and Remote Sensing, Vol. 42, No. 10, October 2004

- [5] V. Peters, S. Knedlik, O. Loffeld. Modelbildung und Simulation eines hochauflösenden 3D-Sensors am Beispiel einer PMD-Kamera. 3D-NordOst 2006 (9. Anwendungsbezogener Workshop zur Erfassung, Modellierung, Verarbeitung und Auswertung von 3D-Daten), Berlin, Germany, December 2006